**Article ID:** 1003－6326(2003)04－0885－05

# Borides at interfacial zone of IC6 TLP bonded joints①

XIE Yong-hui (谢永慧), MAO Wei(毛 唯), LIU Xiao-fang(刘效方), YAN Ming-gao(颜鸣皋)
(Laboratory of Welding and Forging, Beijing Institute of Aeronautical Materials, Beijing 100095, China)

**Abstract:** Transient liquid phase (TLP) bonding technique was used in joining IC6 alloy, a newly developed $Ni_3Al$ based intermetallic material. Studies were focused on the borides at the interfacial zone, which were formed through the diffusion of boron from the interlayer into the base metal during the bonding process. The morphology and microstructure of the borides were investigated, as well as their growth mechanism and microstructure evolution with increasing holding time. Both the needle-like and the blocky borides were testified by EDS and TEM as $Mo_2NiB_2$, with (110) and (211) as interfacial planes. The results show that the borides have some orientation relationship with that of the base metal, that is $(211)_{borides} \parallel (111)_{substrate}$, $\langle\bar{1}11\rangle_{borides} \parallel \langle 1\bar{2}3\rangle_{substrate}$. The growth of the borides is controlled by long-range diffusion of solute atoms. The borides are always enveloped by $\gamma'$-$Ni_3$(Al, Mo) films, which would influence the growth behavior of the borides greatly.

**Key words:** transient liquid phase bonding; borides; $Ni_3Al$ based alloys
**CLC number:** TG 245 **Document code:** A

## 1 INTRODUCTION

Transient liquid phase (TLP) bonding technique has been successfully used in joining heat resistant alloys, like Hastelloy X, Inconel 713C, In100, Udimet 500, 700, Mar－M200, 007, 247, 302, Rene′ 80, TD-NiCr, MA754, 6000, PWA1422, CSMX-2 etc, which are susceptible to hot cracking or post-weld heat-treatment cracking problems during fusion welding[1-4]. In addition, there were reports of joining NiAl and TiAl intermetallics by TLP bonding method[5-10]. For example, Gale had investigated the microstructure of NiAl/NiAl and NiAl/Ni joints in detail, using pure Cu or Ni-4.5Si-3.2B (mole fraction, %) as interlayers respectively. They also developed wide-gap TLP bonding strategies for cast Ti-48Al-2Cr-2Nb (mole fraction, %), using Ti-48Al-2Cr-2Nb/Cu composite interlayer.

In the TLP bonding process, an interlayer containing elements for depressing melting point was inserted between the base metal surfaces. At the bonding temperature, the interlayer melted and filled the joint clearance, then isothermal solidification occurred by interdiffusion between the liquid and the base metal. No liquid would remain in the bonding seam when isothermal solidification ended. By maintaining the joint at the bonding temperature after isothermal solidification, joint with chemical composition and microstructure similar with that of the base metal could be achieved.

IC6 alloy, with the chemical composition of Ni-(7.5－8.5) Al-(13－15) Mo-(0.01－0.1) B (mass fraction, %), is a $Ni_3Al$ based alloy developed by Beijing Institute of Aeronautical Materials (BIAM) for turbine blades and vanes, with the service temperatures ranging from 1 000 ℃ to 1 100 ℃[11]. Joining is an indispensable technique for the application of this material. Some studies had shown that crack-free welds could not be obtained for the cast $Ni_3Al$ materials by fusion welding[12, 13]. However, little research had been reported on TLP bonding of $Ni_3Al$ materials. In order to join IC6 alloy by the TLP bonding method, we designed nickel-based filler metals with 1%－4% (mass fraction) boron added as melting-point-depressant and sound joints were obtained[14]. Due to small molecular size, boron could readily diffuse into the adjoining base metal during the bonding process and a large amount of borides would form at the interfacial zone. In the present paper, the morphology and microstructure of the borides, as well as their growth mechanism and microstructure evolution with increasing holding time are investigated.

## 2 EXPERIMENTAL

Pieces of IC6 alloy of 20 mm in diameter and 3mm in thickness were cut from the ingot, which had been solution treated at 1 250 ℃ for 10 h and cooled in argon gases. The interlayer used was 40 μm thick foils with chemical composition of Ni-(10－15) Cr-(1－4) B (mass fraction, %), whose solidus and liquidus temperature were 1 080 ℃ and

① **Foundation item:** Project (99H21014) supported by the Aeronautical Science Foundation of China
**Received date:** 2002－07－09; **Accepted date:** 2002－12－25
**Correspondence:** XIE Yong-hui, Senior Engineer, PhD Candidate; Tel: +86-10-62458113; E-mail: yonghui_cn@sina.com

1 120 ℃, respectively. The specimen surface to be bonded were mechanically polished by SiC emery paper and then polished with diamond paste, followed by ultrasonical cleaning in acetone and drying in air. The bonding experiments were conducted at 1 220 ℃ in a vacuum furnace in which the vacuum was better than $2 \times 10^{-2}$ Pa, and the holding time ranged from 5 min to 24 h. After bonding, the specimen were sectioned and the analytical surfaces were polished and etched with 30% hydrofluoric acid, 15% nitric acid and 55% glycerin for observations by a JSM-5600 scanning electron microscopy (SEM). In addition, chemical composition of the borides was examined both by Link ISIS300 energy dispersive spectroscopy (EDS) and JXA-8800R electron probe micro-analysis (EPMA). Microstructure of the borides at the interfacial zone was observed by JEM-200CX and H-800 transmission electron microscopy (TEM). Noted, the selected-area diffraction patterns with "*" were photographed by JEM-200CX, while the others were photographed by H-800.

## 3 RESULTS AND DISCUSSION

### 3.1 Chemical composition

The chemical composition of the borides at the bonding interface and the surrounding films examined by EDS and EPMA is shown in Table 1, and the compositions of γ and γ′ phase in the base metal are also listed for comparison. It is evident that the borides are mainly composed of Ni and Mo, with little Cr and Al. The atomic ratio of Ni to Mo is about 1 : 2, indicating that the borides have a chemical formula of $Mo_2NiB_2$. Fig. 1 shows the line scanning composition profile of the borides by EPMA. It can also be clearly seen that the borides are rich in Mo and poor in Al. In consequence, the Mo content of adjoining base metal is reduced, whereas the Al content is increased. As given in Table 1, the films enclosing the borides has a chemical composition of γ′-$Ni_3$(Al, Mo), and the Al content is slightly higher than that of the γ′ phase in the base metal far from the interface.

**Table 1** Chemical compositions of phases in IC6 TLP bonded joint (mass fraction, %)

| Location | Ni | Mo | Al | Cr | B |
|---|---|---|---|---|---|
| Borides | 26.28 | 70.68 | – | 2.80 | 7.30 |
| Films enclosing borides | 84.79 | 7.49 | 6.81 | 0.02 | * |
| γ phase in base metal | 76.21 | 20.14 | 2.25 | – | – |
| γ′ phase in base metal | 80.95 | 12.73 | 5.70 | – | – |

* B could not be detected accurately, but could be estimated by total (100%) minus contents of other elements.

### 3.2 Morphology

Fig. 2 shows the bright-field image and selected-area diffraction(SAD) patterns of the borides observed by TEM. There are mainly two kinds of morphology, needle-like or blocky, and some borides have planar interfaces. By calibrating SAD patterns of $B$ = [001], [100] and [010], we know that the lattice parameters of the borides are in accordance with $Mo_2NiB_2$ listed in Ref. [15], showing that $Mo_2NiB_2$ has a body-centered orthorhombic structure and lattice parameters of $a$ = 7.03 Å, $b$ = 4.74 Å, $c$ = 3.13 Å.

In addition, it is known from the bright-field image and relative SAD patterns that the planar faces corresponds to (110) or (211) planes, as shown in Fig. 3. Since {110} and {112} are the close-packed planes of body-centered cubic metals, it can be estimated that for body-centered orthorhombic structure with lattice parameters $a > b > c$, (110) and (211) pack more closely with larger plane distance. As could be expected, these closely packed planes have lower growth rate, and the morphology of the borides would be determined by the growth rates of the (110) and (211) planes.

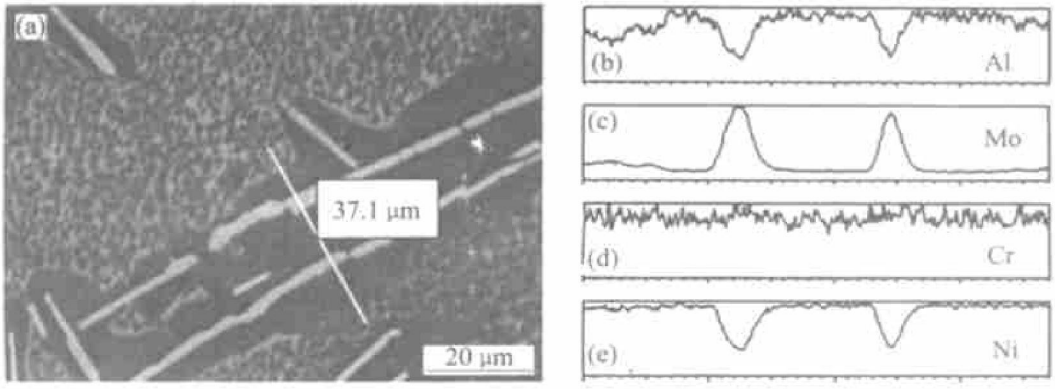


**Fig. 1** Morphology of borides(a) and elemental line scanning composition profiles at interfacial zone by EPMA ((b)~(e))

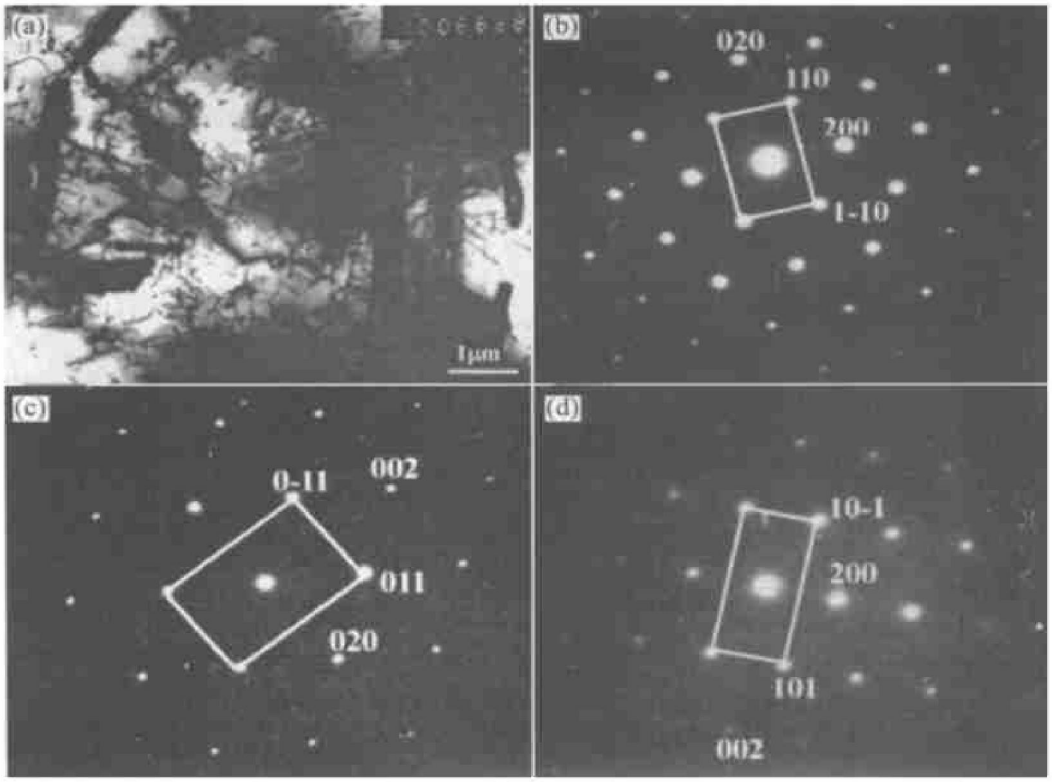


**Fig. 2** TEM bright field image of borides and SAD patterns
(a) —Bright field image; (b) —$B$= [001]; (c) —$B$= [100]; (d) —$B$= [010]

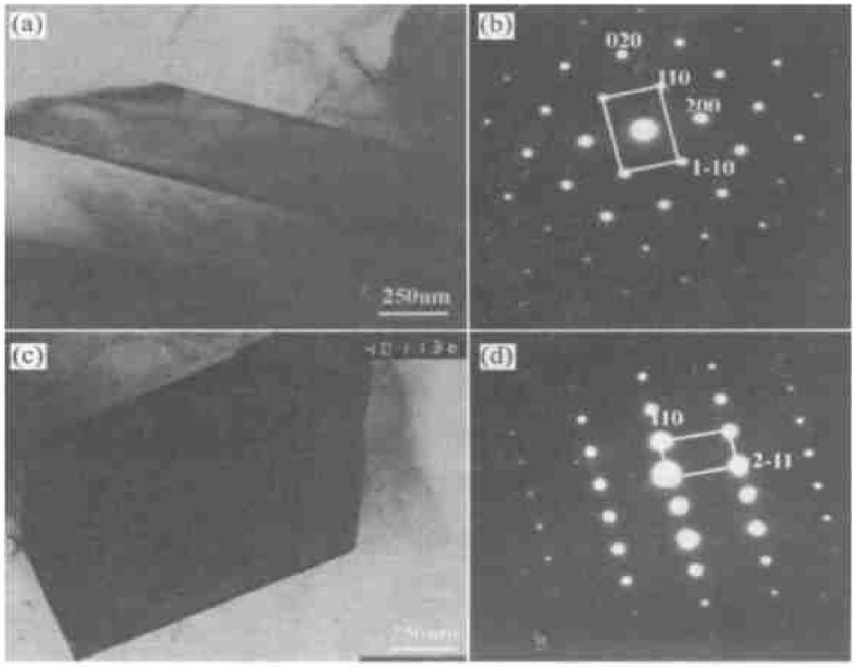


**Fig. 3** Borides and corresponding SAD patterns
(a) —Needle-like borides; (b) —Corresponding $B$= [001]; (c) —Blocky borides; (d) —Corresponding $B$= $[1\,\bar{1}\,\bar{3}]^*$

### 3.3 Growth mechanism

Fig. 4 shows the orientation relationship of the borides with the substrate from SAD patterns, which could be described as $(211)_{\text{borides}} \parallel (111)_{\text{substrate}}$, $\langle\bar{1}11\rangle_{\text{borides}} \parallel \langle12\bar{3}\rangle_{\text{substrate}}$, and (211) plane of the borides has little discompatibility with (111) plane of the $\gamma'$ substrate by calculating their plane distance respectively. As a result, the borides would be parallel to each other, or intersect by certain angles. Since the borides has a wholly different structure and chemical composition with that of the substrate, their formation and growth require two prerequisites. First, the solute atoms should transfer from the base metal to the phase boundaries to satisfy the composition need. Second, the atoms nearby should adjust their

location. Therefore, those planes in the borides like (211), which has good compatibility with the substrate, can reduce the interfacial energy and make the formation of the borides easier. It could be presumed that the borides grow by a terrace mechanism controlled by long range diffusion of solute atoms[16], testified by the small terraces on the surface of the borides in Fig. 5.

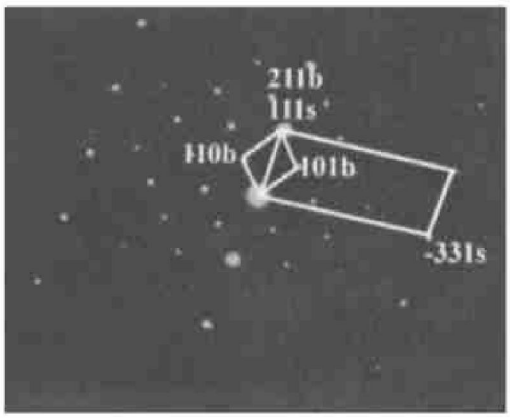


**Fig. 4** Orientation relationship between SAD pattern of borides and substrate*
$((211)_{borides} \parallel (111)_{substrate}, \langle 111\rangle_{borides} \parallel \langle 123\rangle_{substrate}$

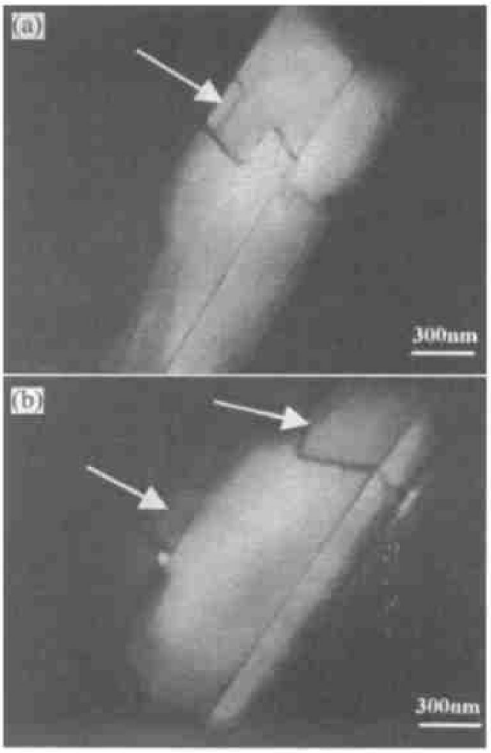


**Fig. 5** Small terraces (as pointed by white arrows) existing on surface of borides
(a) —Needle-like boride; (b) —Blocky boride

### 3.4 Microstructure evolution of borides with increasing holding time

Increasing the holding time from 5 min to 24 h at 1 220 ℃ caused great changes in the morphology, amount and distribution of the borides at the bonding interface, as shown in Fig. 6. When held for 5 min, a lot of borides formed, parallel to each other or intersected by certain angles. When held for 4 h, the borides aggregate and $\gamma'$ films are interconnected. However, as the holding time increases to 24 h, the amount of the borides decreases. Furthermore, $\gamma'$ films become isolated from each other. Schematic explanation is shown in Fig. 7. Since the intersecting point of $\gamma'$ films has a smaller vertex angles, it would result in a higher content of solute according to Gibbs-Tompson's principle[16]. Then the solute, Mo etc would transfer to other places by the driving force of composition grads, making the vertex angles even smaller. Finally, the $\gamma'$ film becomes disconnected and envelopes the borides separately, and then the solute atoms cross the $\gamma'$ film to reach the borides. Because the $\gamma'$ film could hinder the diffusion of Mo element into the borides, the amount and dimension of the borides begin to decrease when the solute could not be supplied enough for their growth, until they disappear completely.

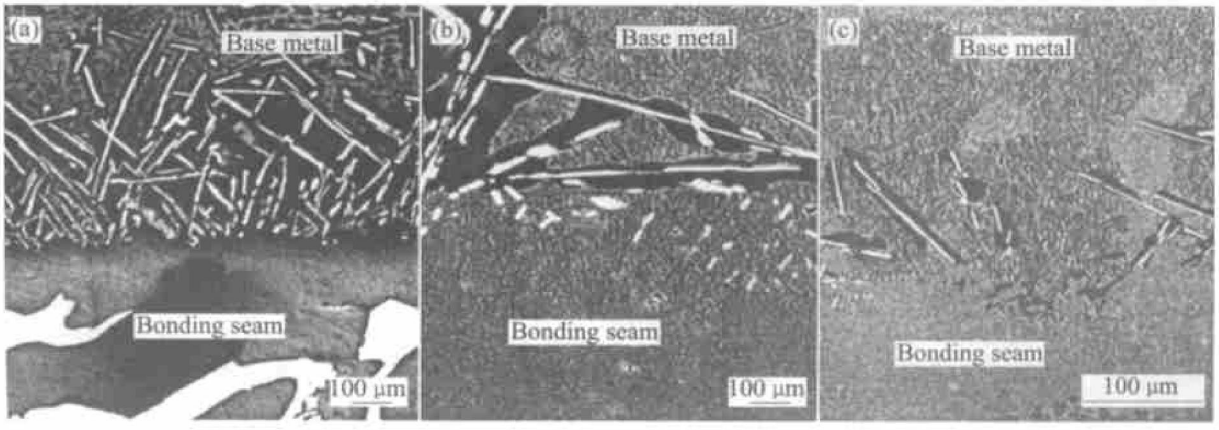


**Fig. 6** SEM photos showing evolution of borides with increasing holding time at 1 220 ℃
(a) —5 min; (b) —4 h; (c) —24 h

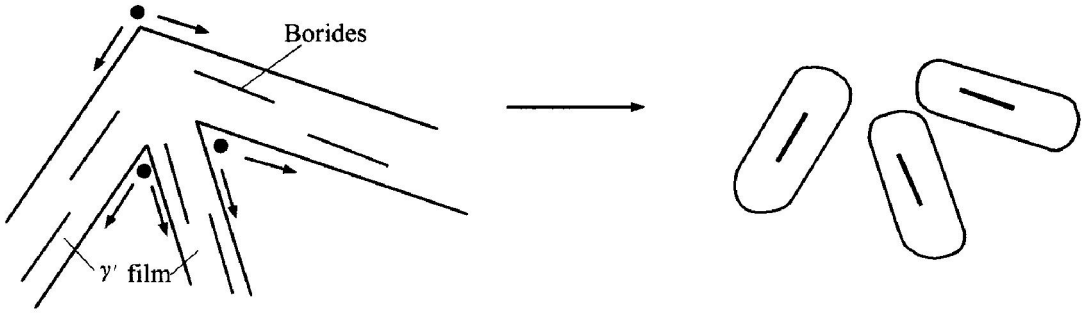


**Fig. 7** Schematic illustration of solute diffusion direction as holding time increases

## 4 CONCLUSIONS

1) The borides have chemical formula of $Mo_2NiB_2$, with a body-centered orthorhombic structure and (110) or (211) as interfacial planes. The borides have some orientation relationship with the substrate, that is, $(211)_{borides} \parallel (111)_{substrate}$, $\langle\bar{1}11\rangle_{borides} \parallel \langle 12\bar{3}\rangle_{substrate}$.

2) The growth of the borides is controlled by long-range diffusion of the solute atoms.

3) As holding time at the bonding temperature increases, the initial interconnecting $\gamma'$ films become disconnected and envelope the borides separately. The amount and dimension of the borides decrease until they disappear completely.

## REFERRENCES

[1] Duvall D S, Owczarski W A. TLP bonding: a new method for joining heat resistant alloys [J]. Welding Journal, 1974, 53(4): 203 - 214.

[2] Cam G, Kocak M. Progress in the joining of advanced materials [J]. International Materials Reviews, 1998, 43(1): 1 - 44.

[3] LI Xiao-hong, MAO Wei. TLP bonding of superalloys [A]. Proceedings of National Symposium on Microjoining and Brazing [C]. Wusi: Welding Institute of Chinese Mechanical Engineering Society, 1994. 19 - 22. (in Chinese)

[4] ZHANG Qi-yun, ZHUANG Hong-shou. Manual of Brazing and Soldering [M]. Beijing: Mechanical Industry Press, 1998. 229 - 241. (in Chinese)

[5] GUAN Y, Gale W F. Transient liquid phase bonding of a Hf bearing single crystal nickel aluminide to MM247 superalloy [J]. Materials Science and Technology, 1999, 15(2): 207 - 212.

[6] Gale W F, WEN X. $Ni_3Al$ based composite interlayers for transient liquid phase bonding of a NiAl-Hf single crystals to a nickel base superalloy [J]. Materials Science and Technology, 2001, 17(4): 459 - 464.

[7] Orel S V, Parous L C, Gale W F. Diffusion brazing of nickel aluminides [J]. Welding Journal, 1995, 9: 319 - 324.

[8] Gale W F, Orel S V. A microstructure investigation of NiAl/ Ni-Si-B / NiAl transient liquid phase bonds [J]. Journal of Material Science, 1996, 31: 345 - 349.

[9] Gale W F, GUAN Y. Transient liquid-phase bonding in the NiAl/ Cu / Ni system —A microstructural investigation [J]. Metall Mater Trans, 1996, 27A(11): 3621 - 3629.

[10] Gale W F, Y XU, X WEN. Wide gap transient liquid phase bonding of Ti-48Al-2Cr-2Nb [J]. Metall Mater Trans, 1999, 30A(10): 2723 - 2726.

[11] LI S H, HAN Ya-fang, MA Sheng, et al. Investigation on cast $Ni_3Al$ base superalloy IC6 [J]. Journal of Aeronautical Materials, 1993, 13(1): 5 - 11. (in Chinese)

[12] Maguire M C, Edwards G R, David S A. Weldability and hot ductility of chromium-modified $Ni_3Al$ alloys [J]. Welding Journal, 1992, 7: 231 - 242.

[13] Santella M L, Horton J A, David S A. Welding behavior and microstructure of a $Ni_3Al$ alloy [J]. Welding Journal, 1988, 3: 3 - 69.

[14] LI Xiao-hong, MAO Wei, CHENG Yao-yong. Microstructures and properties of transient liquid phase diffusion bonded joints of $Ni_3Al$-base superalloys [J]. Trans Nonferrous Met Soc China, 2001, 11(3): 405 - 408.

[15] JIN Yan, HAN Ya-fang, Chaturvedi M C. Crystallographic analysis of the borides in the $Ni_3Al$ base alloy IC6 [J]. Materials Science and Engineering, 1995, A202: 193 - 200.

[16] FENG Duan. Physical Metallurgy [M]. Beijing: Science Press, 1998. 111 - 216. (in Chinese)

**(Edited by LONG Huai-zhong)**